Available online at www.sciencedirect.com

SCIENCE DIRECT

Developmental Biology 277 (2005) 255–269

DEVELOPMENTAL BIOLOGY

www.elsevier.com/locate/ydbio

Distinctive functions of membrane type 1 matrix-metalloprotease (MT1-MMP or MMP-14) in lung and submandibular gland development are independent of its role in pro-MMP-2 activation

Samantha A. Oblander[a], Zhongjun Zhou[b], Beatriz G. Gálvez[c], Barry Starcher[d], John M. Shannon[e], Madeleine Durbeej[f], Alicia G. Arroyo[c], Karl Tryggvason[g], Suneel S. Apte[a,*]

[a]*Department of Biomedical Engineering, Lerner Research Institute, Cleveland Clinic Foundation, Cleveland, OH, United States*
[b]*Department of Biochemistry, University of Hong Kong, Hong Kong, China*
[c]*Nacional de Investigaciones Cardiovasculares, Madrid, Spain*
[d]*University of Texas Health Center at Tyler, Tyler, TX, United States*
[e]*Cincinnati Children's Hospital Medical Center, Cincinnati, OH, United States*
[f]*Department of Cell and Molecular Biology, Lund University, Lund, Sweden*
[g]*Matrix Biology and Biochemistry, Karolinska Institute, Stockholm, Sweden*

Received for publication 19 April 2004, revised 26 September 2004, accepted 27 September 2004

Abstract

Membrane type 1-matrix metalloprotease (MT1-MMP or MMP-14) is a major activator of pro-MMP-2 and is essential for skeletal development. We show here that it is required for branching morphogenesis of the submandibular gland but not the lung. Instead, in the lung, it is essential for postnatal development of alveolar septae. Lung development in *Mmp14−/−* mice is arrested at the prealveolar stage with compensatory hyperinflation of immature saccules. *Mmp2−/−* mice lacked comparable defects in the lung and submandibular gland, suggesting that MT1-MMP acts via mechanisms independent of pro-MMP-2 activation. Since the developmental defects in the lung are first manifest around the time of initial vascularization (E16.5), we investigated the behavior of pulmonary endothelial cells from *Mmp14+/+* and *Mmp14−/−* mice. Endothelial cells from lungs of 1-week-old *Mmp14−/−* mice show reduced migration and formation of three-dimensional structures on Matrigel. Since pulmonary septal development requires capillary growth, the underlying mechanism of pulmonary hypoplasia in *Mmp14−/−* mice may be defective angiogenesis, supporting a model in which angiogenesis is a critical rate-limiting step for acquisition of pulmonary parenchymal mass.

Keywords: MT1-MMP; Branching morphogenesis; Alveolization; Lung; Submandibular gland; Angiogenesis; MMP; TIMP; Septation; Pulmonary

Introduction

The development of epithelial organs such as the lung, submandibular gland, breast, liver, and kidney involves complex interactions between epithelial and stromal cells, the developing vasculature, and the surrounding extracellular matrix (ECM) (Affolter et al., 2003; Kanwar et al., 2004; Warburton et al., 2000). In this context, ECM and ECM-degrading proteases provide major environmental influences, affecting cell migration, proliferation, differentiation, attachment, and apoptosis (Blavier and Delaisse, 1995; Giannelli et al., 1997; Simian et al., 2001; Werb, 1997). Typically, proteases are highly regulated by transcriptional regulation, zymogen activation, cell/tissue compartmentalization, and secreted inhibitors, and they often have restricted substrate specificity. For these reasons, it is likely that individual proteases may be required at distinct

* Corresponding author. Department of Biomedical Engineering, Lerner Research Institute, Cleveland Clinic Foundation (ND-20), 9500 Euclid Avenue, Cleveland OH, 44195. Fax: +1 216 444 9198.
E-mail address: aptes@ccf.org (S.S. Apte).

0012-1606/$ - see front matter © 2004 Elsevier Inc. All rights reserved.
doi:10.1016/j.ydbio.2004.09.033

stages of organ development or for specific events and processes in their morphogenesis. Historically, one of the major classes of proteases in the developmental context are matrix metalloproteases (MMPs), which constitute a large family of Zn^{2+}- and Ca^{2+}-dependent enzymes (Somerville et al., 2003; Werb, 1997). These proteases are synthesized as zymogens, and following activation, they are regulated by tissue inhibitors of metalloproteinases (TIMPs). MMPs have been implicated in the development of epithelial organs by a variety of experimental approaches. For instance, synthetic and natural metalloprotease inhibitors have been shown to influence developmental processes in vitro and in vivo (Alexander et al., 1996; Ganser et al., 1991; Simian et al., 2001; Wiseman et al., 2003). Such inhibitors typically inhibit not just one, but a number of MMPs. Furthermore, MMP inhibitors can affect a larger constituency of proteases than is usually considered, such as metalloproteases of the ADAM and ADAMTS families. Another approach, overexpression of metalloproteases in transgenic mice, has provided insight into what proteases can do (D'Armiento et al., 1992; Sympson et al., 1994; Witty et al., 1995), but not necessarily into what individual enzymes actually do in vivo. Surprisingly, inactivation of individual MMP genes in mice suggested that many MMPs have modest developmental roles (Parks and Shapiro, 2001; Somerville et al., 2003) since the null mice have not shown obvious developmental defects. However, careful analysis is beginning to uncover physiological functions using these genetic models (Wiseman et al., 2003).

MMPs exist as both secreted and membrane-bound forms. The membrane-type MMPs (MT-MMPs) are anchored to the cell surface through a membrane-spanning segment or a glycosylphospatidylinositol (GPI) anchor (Yana and Seiki, 2002; Zucker et al., 2003). Membrane type 1 (MT1)-MMP (or MMP-14)[1], a type I transmembrane protein (Sato et al., 1994), is the most extensively studied of the six cell-surface MMPs. *Mmp14* is subject to a high degree of temporal and spatial transcriptional regulation during development (Apte et al., 1997; Kinoh et al., 1996). Transcriptional regulation is especially significant in the case of MT1-MMP since, like the other MT-MMPs, its prodomain is constitutively removed by proprotein convertases (e.g., furin) in the secretory pathway, resulting in delivery of catalytically active enzyme at the cell surface (Sato et al., 1996; Yana and Weiss, 2000). Although it can degrade molecules such as collagen I, laminin, fibrin, and fibronectin (Hotary et al., 2002; Ohuchi et al., 1997), MT1-MMP is better known as the cell-surface activator of pro-MMP-2 (also known as progelatinase A) (Sato et al., 1994). MMP-2 has long been thought to be an important protease in the context of development. Mutations in human MMP-2 cause a multicentric osteolysis and arthritis syndrome (Martignetti et al., 2001). Unlike MT1-MMP, MMP-2 is secreted as a zymogen, pro-MMP-2. The pro-MMP-2 activation process requires the formation of a trimolecular complex in which TIMP-2 links MT1-MMP to MMP-2 (Sato et al., 1994; Strongin et al., 1995). Previous studies describing coordinated developmental expression of *Mmp14*, *Mmp2*, and *Timp2* (Apte et al., 1997; Kinoh et al., 1996) seemed to underscore the essential role of MT1-MMP and TIMP-2 in pro-MMP-2 activation and suggested that MMP-2 was critical for development. Neither *Mmp2−/−* nor *Timp2−/−* mice, however, have major developmental anomalies (Itoh et al., 1997; Wang et al., 2000), while *Mmp14−/−* mice have the most striking developmental phenotype of all null MMP alleles. Their phenotype consists of postnatal dwarfism, musculoskeletal defects including reduced growth plate proliferation, and defective vascular invasion of the skeleton. *Mmp14−/−* mice usually die by 3 weeks of age of unknown causes (Holmbeck et al., 1999; Zhou et al., 2000). MT1-MMP also activates collagenase-2 or MMP-13 (Knauper et al., 2002), which is primarily expressed in the developing skeleton in mice and humans (Blavier and Delaisse, 1995; Johansson et al., 1997).

Here, *Mmp14−/−* mice are shown to have defects in the lung and submandibular gland, suggesting an essential role for MT1-MMP in development of these epithelial organs. Lack of MT1-MMP substantially affects branching morphogenesis in vitro in the submandibular gland, but not in the lung. Instead, in the lung, MT1-MMP has a major role in the postnatal development of the alveolar septum, whose function is to dramatically increase the pulmonary surface area available for exchange of respiratory gases. Septal extension requires capillary growth, and in addition to defective angiogenesis previously noted in *Mmp14−/−* mice, we specifically show here that lung endothelial cells are defective in migration and fail to form three-dimensional structures on a Matrigel substratum. We propose that failed septation is a consequence of impaired angiogenesis in *Mmp14−/−* mice. *Mmp2−/−* mice are shown not to have comparable anomalies, suggesting that MT1-MMP acts in these contexts via mechanism(s) independent of pro-MMP-2 activation.

Materials and methods

Mmp14 and Mmp2 transgenic mice

Mice with inactivated *Mmp14* (MT1-MMP) alleles have been described previously (Zhou et al., 2000) and were maintained in the C57/BL6 strain. Crosses of heterozygous (+/−) mice were established to produce *Mmp14−/−* and +/+ littermates of various embryonic and postnatal ages. The morning of the day, a vaginal plug was detected was designated as E0.5. *Mmp2−/−* mice (C57/BL6) were kindly

[1] Since MT1-MMP is generally used in the literature to describe MMP-14 protein, we have used this term throughout the paper. However, when referring to the genes we have used the approved gene nomenclature, for example, *Mmp14* and *Mmp2*.

provided by Dr. Shigeyoshi Itohara and have been described previously (Itoh et al., 1997). Genotyping of the *Mmp14* and *Mmp2* mouse strains was performed by PCR.

Routine histology, immunohistochemistry, in situ hybridization, and three-dimensional histological construction

Unless obtained from embryos, lungs were always fixed under inflation by intratracheal infusion of fixative as well as by immersion in the fixative. Tissues were fixed in 10% formalin, 4% paraformaldehyde, or Histochoice™ according to the specific application and embedded in paraffin. Alternatively, tissue was also frozen in OCT for cryosectioning. Sections (5–7 μm thick) were stained with hematoxylin and eosin (H and E), the Movat pentachrome stain, and modified Hart's stain for elastin. Immunohistochemistry utilized antibodies to elastin, von Willebrand factor (vWF) (Dako), PECAM/CD31 (Pharmingen), surfactant protein B (Chemicon), Clara cell-secreted protein (provided by Dr. Barry Stripp), and smooth muscle α-actin (Dako). In situ hybridization of digoxigenin or radioactive cRNA probes to cryosections or paraffin sections, respectively, was done as previously described (Albrecht et al., 1997). Surfactant protein C (Spc) cRNA probes were radiolabeled prior to in situ hybridization as previously described (Deterding and Shannon, 1995). H and E stained sections were used to determine the mean linear intercept in *Mmp14−/−* and *Mmp14+/+* mice, and statistical analysis by *t* test for paired data was done using a computer software package (InStat, Graph Pad, San Diego, CA).

For three-dimensional reconstruction of the E18.5 bronchial tree, *Mmp14−/−* and *Mmp14+/+* littermate lungs were inflation-fixed in 10% formalin. The periphery of the lungs was then reconstructed from imaging 5-μm serial sections using proprietary histological technology and analytical software (Resolution Sciences, Corte Madera, CA, now defunct). The prospective airspaces were constructed by ascribing a solid volume to all spaces that were devoid of tissue. Subsequently, all stained tissue was subtracted, leaving behind a "virtual corrosion cast" of the lung periphery. Desmosine analysis was performed on lung hydrolysates as previously described (Starcher and Conrad, 1995).

Scanning (SEM) and transmission electron microscopy (TEM)

Lungs from 2-week-old *Mmp14−/−* and *Mmp14+/+* littermate mice were fixed by intratracheal perfusion with 1.25% glutaraldehyde in PBS under inflation and immersed further in the same fixative for 4 h, dehydrated, and sputter-coated with gold at a rate of 3 A°/s (SPI-Module Sputter Coater, SPI Supplies, Inc). Specimens for SEM were viewed under a Jeol JSM-5310 scanning electron microscope. Specimens for TEM were fixed as for SEM, washed with cold sodium cacodylate buffer (0.2 M, pH 7.3) three times for 5 min each, osmicated using 1% osmium tetroxide in water for 1 h, and rinsed twice in cacodylate buffer and maleate buffer, followed by staining with 1% uranyl acetate. Specimens were dehydrated and embedded in LX-112 medium. Thick (1 μm) sections were prepared for light microscopy by staining with toluidine blue, and thin sections (80 nm) were mounted on formvar-coated grids for viewing under a Phillips electron microscope at 80 kV.

In vitro organ culture

Lung rudiments dissected from E12.5 *Mmp14−/−* and +/+ embryos were cultured for 72 h on porous membranes (8-μm pore size, Nucleopore, Whatman) in 24-well plates. Cultures were maintained at 37°C in 95% air, 5% CO_2 in 1 ml of Dulbecco's modified Eagle medium, nutrient mixture F-12 (1:1, Gibco BRL) supplemented with 0.03 mM sodium bicarbonate, 10 μg/ml apo-transferrin, 1 μg/ml BSA, and 50 μg/ml gentamicin. Lungs were then photographed using a Sony CCD-IRIS color video camera attached to an Olympus microscope. Branching morphogenesis was quantitated from 0 to 72 h by counting the number of terminal end buds. Some lung rudiment cultures were done in medium supplemented in addition to the above, with 2% or 10% FBS.

E13.5 submandibular gland rudiments were grown on a porous membrane (5-μm pore size, Nucleopore, Whatman), supported by a plastic grid and cultured with improved minimum essential medium (IMEM-ZO) supplemented with 50 μg/ml transferrin (BD Biosciences). Branching morphogenesis was quantitated at 12-, 24-, 48-, and 72-h intervals by counting the number of terminal end buds.

Gelatin zymography and Western blotting

Lung or submandibular gland tissue from *Mmp14−/−* and +/+ littermate mice was homogenized in cold lysis buffer (50 mM Tris–HCl pH 7.6, 150 mM NaCl, 5 mM $CaCl_2$, 10 mM EDTA, and 0.02% Tween), incubated on ice for 30 min, and centrifuged at 10,000 rpm for 10 min at 4°C. Protein samples (100 μg) were incubated with 100 μl gelatin sepharose (Amersham Pharmacia), mixed at 4°C for 2 h, and centrifuged at 8000 rpm for 5 min. Thirty microliters of the gelatin sepharose beads was electrophoresed on a 10% SDS–PAGE gel containing 1 mg/ml gelatin (Bio-Rad). The gel was washed twice (30 min each) with 2.5% Triton X-100 and then ddH_2O, incubated for 48 h in MMP buffer (50 mM Tris–HCl pH 7.4, 200 mM NaCl, 20 mM $CaCl_2$) at 37°C, stained with Simply Blue Safestain (Invitrogen) for 1 h, and destained in ddH_2O for 8 h, prior to drying using Dry Ease mini gel drying kit (Invitrogen). For Western blotting, lung protein extracts were separated by SDS–PAGE and transferred to a nitrocellulose membrane (BioTrace™ NT;

Pall Gelman Laboratory). After blocking the membrane with 10% fat-free dry milk in Tris-buffered saline, the membrane was probed with anti-laminin-5 γ2 chain rat polyclonal antibody (Pyke et al., 1995) and antibodies to collagen IV. Anti-actin polyclonal antibody was used as a control to ensure equal loading. Protein was visualized on Kodak Biomax chemiluminescent film using ECL Western Blot Detection reagent (Amersham Pharmacia).

Mouse lung endothelial cells (MLECs) isolation

Lungs from *Mmp14−/−*, *Mmp14+/−*, and *Mmp14+/+* C57BL/6J mice were excised with sharp scissors, digested with 0.1% collagenase for 1 h at 37°C (Worthington), and further disaggregated to produce a single cell suspension. The mixed population obtained was subjected to negative selection with anti-CD16 (BD Biosciences)-coated magnetic beads (Dynal) and then to positive selection with anti-ICAM-2 (BD Biosciences)-coated magnetic beads, which resulted in a >90% pure population of endothelial cells. MLECs were grown on a mixture of 10 mg/ml fibronectin (Sigma), 10 mg/ml vitrogen (Cohesion), and 0.1% gelatin (Sigma)-coated 75-cm flasks (Costar Corp.) with DMEM (low glucose), Ham's F-12 (Gibco), 20% FBS, heparin (Sigma), endothelial mitogen (Biogenesis), glutamine (Sigma), and antibiotics. The cells were used for up to four passages. MT1-MMP expression was tested in MLEC lysates by Western blotting with the anti-MT1-MMP mAb LEM-2/63 (Galvez et al., 2001).

Cell transmigration assay

MLEC transmigration assays were performed in 8-μm pore transwell chambers (Costar Corp.). Cells were resuspended in serum-free medium (Gibco-BEL Life Sciences) and seeded at 15,000 cells/well on matrigel-coated filters (Fisher) in the upper chamber. Cells that had migrated onto the lower surface of the filter were stained with toluidine blue (Sigma) and counted after 5 h of migration. Experiments were done in duplicate, and four fields of each transwell were counted with a 40× objective under a microscope.

In vitro endothelial morphogenesis assay

Matrigel basement membrane matrix (Becton-Dickinson) was diluted 1:2 in cold DMEM medium (Gibco). Diluted Matrigel (80 μl) was plated into flat-bottomed 96-well tissue culture plates (Costar Corp.) and allowed to gel for 20 min at 37°C before cell seeding. Then, 4×10^4 cells were added atop the Matrigel. After 4-h incubation, cord-like and tube-like structures were counted with a 40× objective microscope in four independent fields in each well. Experiments were done in duplicate. Statistical analysis was done using a Student *t* test for paired samples.

Results

Mmp14−/− mice have defective alveolar septal development

Mmp14−/− mice were born in the expected mendelian ratio. Of 52 *Mmp14* heterozygote crosses (in the C57/BL6 strain) used in this study, 116 of the progeny (30%) were homozygous for the wild-type allele, (*Mmp14+/+*), 178 (45%) were heterozygous (*Mmp14+/−*), and 98 (25%) were homozygous null (*Mmp14−/−*). This approximately 1:2:1 ratio confirms that the null genotype does not cause embryonic lethality or that it does so very rarely. In addition, we also bred the null allele into the FVB and Swiss Webster strains for eight generations and found anomalies essentially similar to those described here and in a previous publication (Zhou et al., 2000). The data shown are all from the C57/BL6 mice.

Because virtually all of our *Mmp14−/−* mice die between 2 and 3 weeks of age, we initially analyzed their lungs at 2 weeks. *Mmp14+/−* lungs were indistinguishable from those of *Mmp14+/+* mice in all aspects of the morphological findings reported here and are not discussed further except in the context of studies on endothelial cells. Lungs from *Mmp14−/−* mice had normal primary branching, that is, one left lobe and four right lobes, but they were considerably smaller than those of +/+ (Fig. 1A) or +/− mice at 2 weeks of age, consistent with the overall growth retardation in these mice. In addition to being smaller, *Mmp14−/−* lungs had increased peripheral transparency (Fig. 1A, inset) and showed surface bullae upon inflation, suggesting hyperinflation of the peripheral air spaces and attenuation of the parenchymal walls at the pleural surface.

Scanning electron microscopy (SEM) of the lung interior at 2 weeks of age demonstrated enlarged air saccules in *Mmp14−/−* lungs (Fig. 1B, right panel). The intervening walls were thinner in *Mmp14−/−* mice and lacked the rounded, thick, free edges visible in *Mmp14+/+* lungs (Fig. 1B, left panel). The interior of the bronchial tubes visualized by scanning electron microscopy (SEM) appeared normal, including the presence of Clara cells (not shown).

Paraffin and plastic-embedded histology, following fixation under inflation at 2 weeks of age, was consistent with the SEM observations, showing enlarged air spaces as well as thinner intervening walls in *Mmp14−/−* mice (Fig. 1C, right panel). In *Mmp14−/−* mice, air spaces had smooth walls compared to the normal, irregularly corrugated walls of alveoli in *Mmp14+/+* mice (Fig. 1C, left panel). Whereas secondary septae (defined as extensions of lung parenchyma with free edges) were obvious in *Mmp14+/+* mice, very few were seen in *Mmp14−/−* mice (Fig. 1C). When present in *Mmp14−/−* mice, secondary septae were short and triangular in cross-section (Fig. 1C). The mean linear intercept value, a quantitative measure of tissue density in the lung, was compared using histological sections of *Mmp14−/−* and *Mmp14+/+* lungs. These values were 26.87 and 47.65 in *Mmp14−/−* and

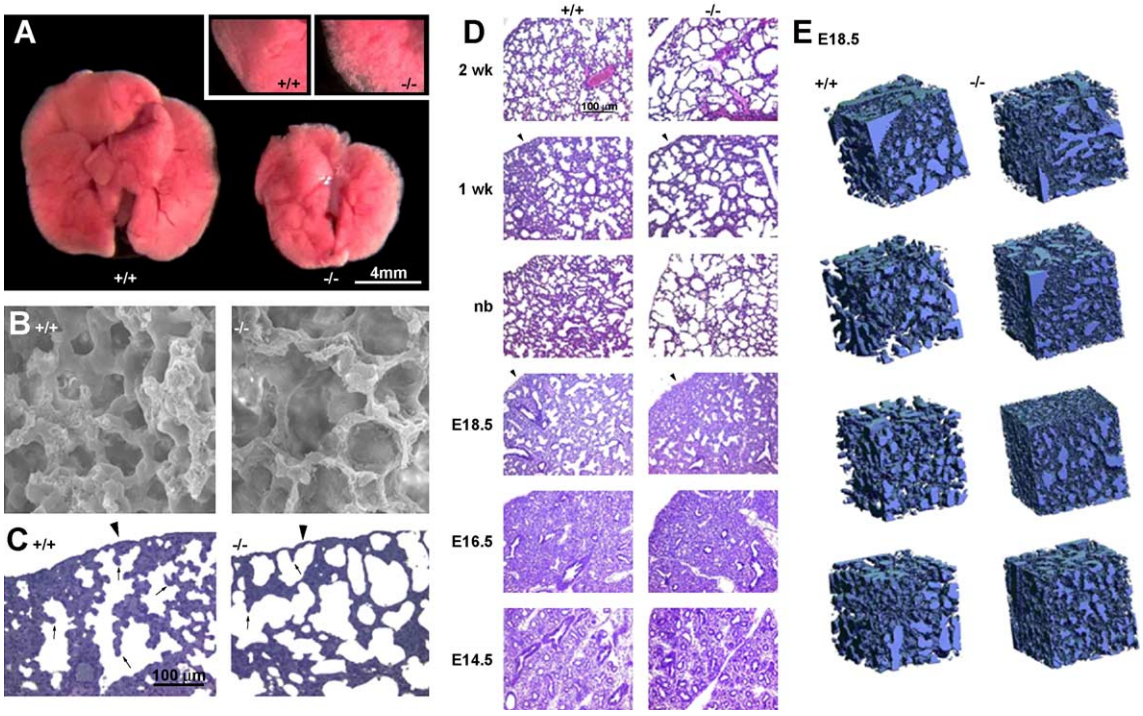

Fig. 1. Abnormal morphology of *Mmp14−/−* lungs at 2 weeks of age. (A) Gross appearance shows decreased size of the *Mmp14−/−* lung, as well as translucency of the periphery (inset higher magnification) hinting at enlarged air spaces. (B) Scanning electron microscopy (×1500 magnification). Air spaces in *Mmp14−/−* mice are dilated with thinner walls between them. Note the rounded edges in *Mmp14+/+* lungs and the smaller air spaces of the normal lung. (C) Light microscopy of toluidine blue-stained, plastic-embedded sections. The arrows indicate septae, and the arrowheads indicate the pleural surface of the lung. (D) Hematoxylin and eosin (H and E)-stained, paraffin-embedded sections of *Mmp14+/+* (left) and *Mmp14−/−* lung (right) from E12.5 to 2 weeks postnatal (×20 magnification). The arrowheads indicate the pleural surface of the lung at E18.5 and 1 week of age. (E) Comparative anatomy of the bronchial tree of the E18.5 *Mmp14+/+* (left) and *Mmp14−/−* (right) mice obtained by three-dimensional reconstruction as explained in Materials and methods. Four representative blocks from each are illustrated.

Mmp14+/+ mice, respectively, and were statistically significant ($P = 0.001$). The peripheral (subpleural) region of the lung was thinner in *Mmp14−/−* mice (Fig. 1C, right panel) and probably explains why bullae were seen on the surface of the inflated *Mmp14−/−* lung.

To track the developmental chronology of these morphological changes noted at 2 weeks of age, we obtained histology at earlier postnatal time points (newborn, 2 days and 1 week, $n = 4$ each time point). Histological abnormalities similar to those in 2-week-old lungs were also consistently present in newborn, 2-day old (not shown), and 1-week-old *Mmp14−/−* mice (Fig. 1D). Since secondary septae are formed postnatally, the histological observations suggested that failure to form secondary septae and subsequent lack of alveolization were the principal problems in lung development of *Mmp14−/−* mice.

Mmp14 is expressed during lung embryogenesis but has a temporally restricted role during late branching morphogenesis

From embryo (E)12.5 to E15.5 days of development, the *Mmp14−/−* lungs were histologically indistinguishable from *Mmp14+/+* lungs (Fig. 1D). From E16.5 days onwards, histological sections showed a relative paucity of bronchial tubes at the periphery of the lung (Fig. 1D). We further delineated the structure of the bronchial tree by three-dimensional reconstruction of tubular structures in the periphery of the lung at E18.5 days (Fig. 1E) showing thinner distal bronchioles in *Mmp14−/−* than in the *Mmp14+/+* mice. This suggested a subtle defect in expansion of peripheral bronchi starting around E16.5.

In situ hybridization demonstrated expression of *Mmp14* in bronchial epithelium throughout embryonic lung development, as shown, for example, at E14.5 and E17.5 (Fig. 2A). *Mmp14* expression was localized to distinct areas consistent with observations that ECM proteolysis during branching morphogenesis occurs in a highly regulated fashion (Wiseman et al., 2003). To elicit the specific role for MT1-MMP in lung branching morphogenesis, we isolated E12.5 lung rudiments from *Mmp14−/−* and *Mmp14+/+* mice and cultured them in serum-free medium for 3 days (Serra et al., 1994), monitoring branching by counting the end buds. *Mmp14+/+* and *Mmp14−/−* lung explants were indistinguishable at E12.5. After 3 days of continued development in culture, there was no consistent morphological difference between *Mmp14+/+* and *Mmp14−/−* lung explants (Fig. 2B). Equal numbers of end buds were counted in matched pairs of lungs ($n = 8$)

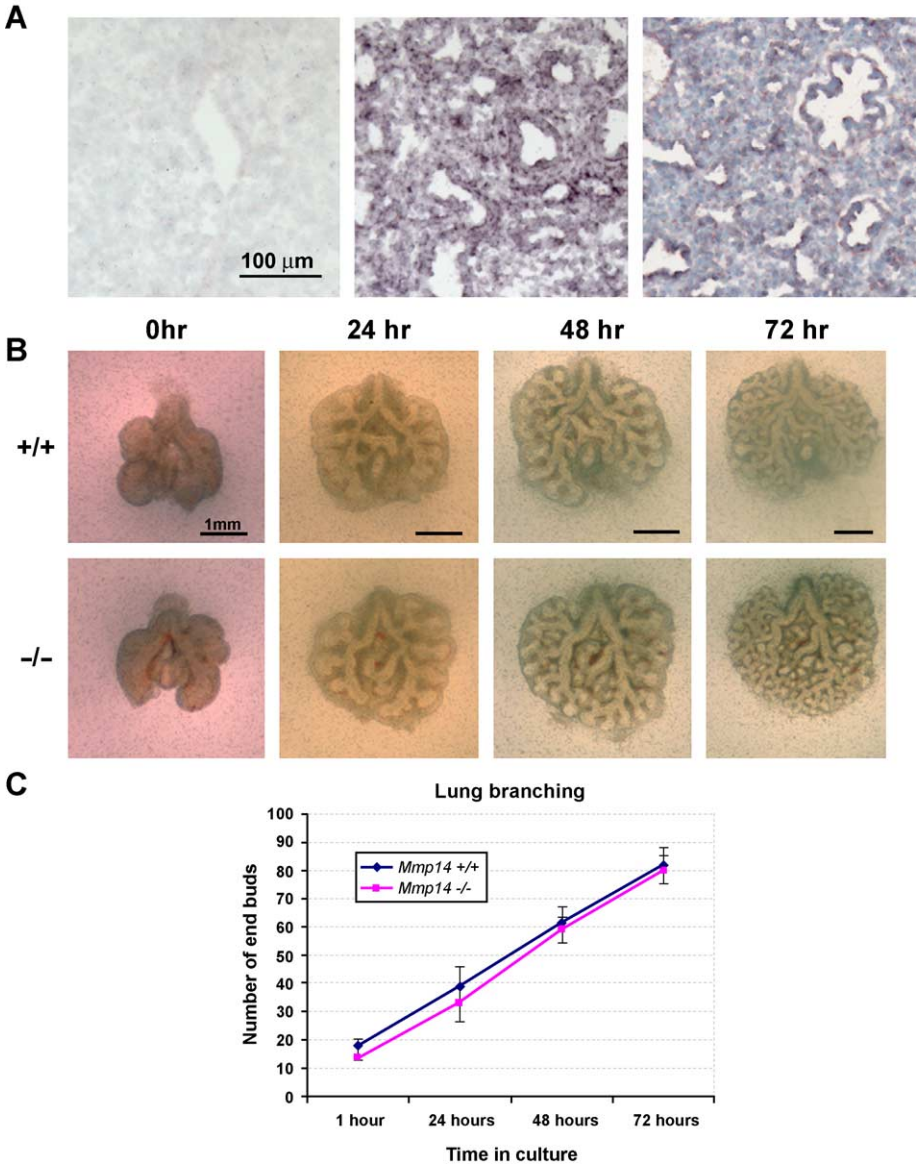

Fig. 2. *Mmp14* is expressed in branching bronchial epithelium, but branching morphogenesis is unaffected in the *Mmp14*−/− lung. (A) In situ hybridization of *Mmp14* expression in mouse lung showing lack of sense probe hybridization (left) and hybridization of antisense probe to E14.5 lung (middle panel) and E17.5 lung (right panel). (B) In vitro branching morphogenesis assay starting at E12.5 and terminated after 72 h. The top row shows a representative result obtained from *Mmp14*+/+ mice, while the lower row shows development of a lung from an *Mmp14*−/− littermate. (C) End buds were counted every 24 h during the branching morphogenesis assay for quantitative evaluation of branching morphogenesis. Blue and red lines indicate *Mmp14*+/+ and *Mmp14*−/−, respectively.

(Fig. 2C) indicating that MT1-MMP was not essential for branching morphogenesis up to E15.5. To determine whether acceleration of branching morphogenesis by addition of serum would uncover a subtle role for MT1-MMP, we repeated these experiments in the presence of 2% or 10% fetal bovine serum. No differences were seen between *Mmp14*+/+ and *Mmp14*−/− lungs ($n = 5$), despite the fact that branching morphogenesis was accelerated in all explants in the presence of serum (data not shown). Based on these experiments and histological observations, we concluded that, although it is expressed in bronchial epithelium, *Mmp14* has a largely redundant role in lung development between E12.5 and E15.5, being required for a temporally specific, relatively minor role in distal bronchiolar expansion after E16.5.

Normal extracellular matrix and cell differentiation in Mmp14−/− lungs

Since one of the demonstrated functions for MT1-MMP is remodeling of the extracellular matrix, we used transmission electron microscopy (TEM) to examine the basement membranes at the gas–blood interface and the cellular composition of the pulmonary parenchyma at 2 weeks of age. The basement membrane at the gas–blood exchange surface was of comparable thickness in *Mmp14*+/+ and

Mmp14−/− mice (Fig. 3A). Both types I and II pneumocytes could be visualized in *Mmp14+/+* and *Mmp14−/−* mice (Fig. 3B). Type II cells in the *Mmp14−/−* mice contained lamellar bodies and demonstrated extrusion of their contents (surfactant) at the cell surface as in the *Mmp14+/+* mice. The developing septae in *Mmp14−/−* mice were blunted, but like those of *Mmp14+/+* mice, they contained a capillary as well as an elastic fiber at the tip (Fig. 3C).

Both TEM (Fig. 3C) and modified Hart's stain (Fig. 4A) showed elastin to be present in developing septae, alveolar walls, and the pleural surface of the lung (Fig. 4A). Quantitative comparison of desmosine cross-links in paired littermates as an indicator of elastin content provided values of 318 ± 121 pM desmosine/mg of total protein in *Mmp14+/+* mice (n = 5) and 262 ± 35 pM desmosine/mg of total protein in *Mmp14−/−* littermates (n = 5). A paired

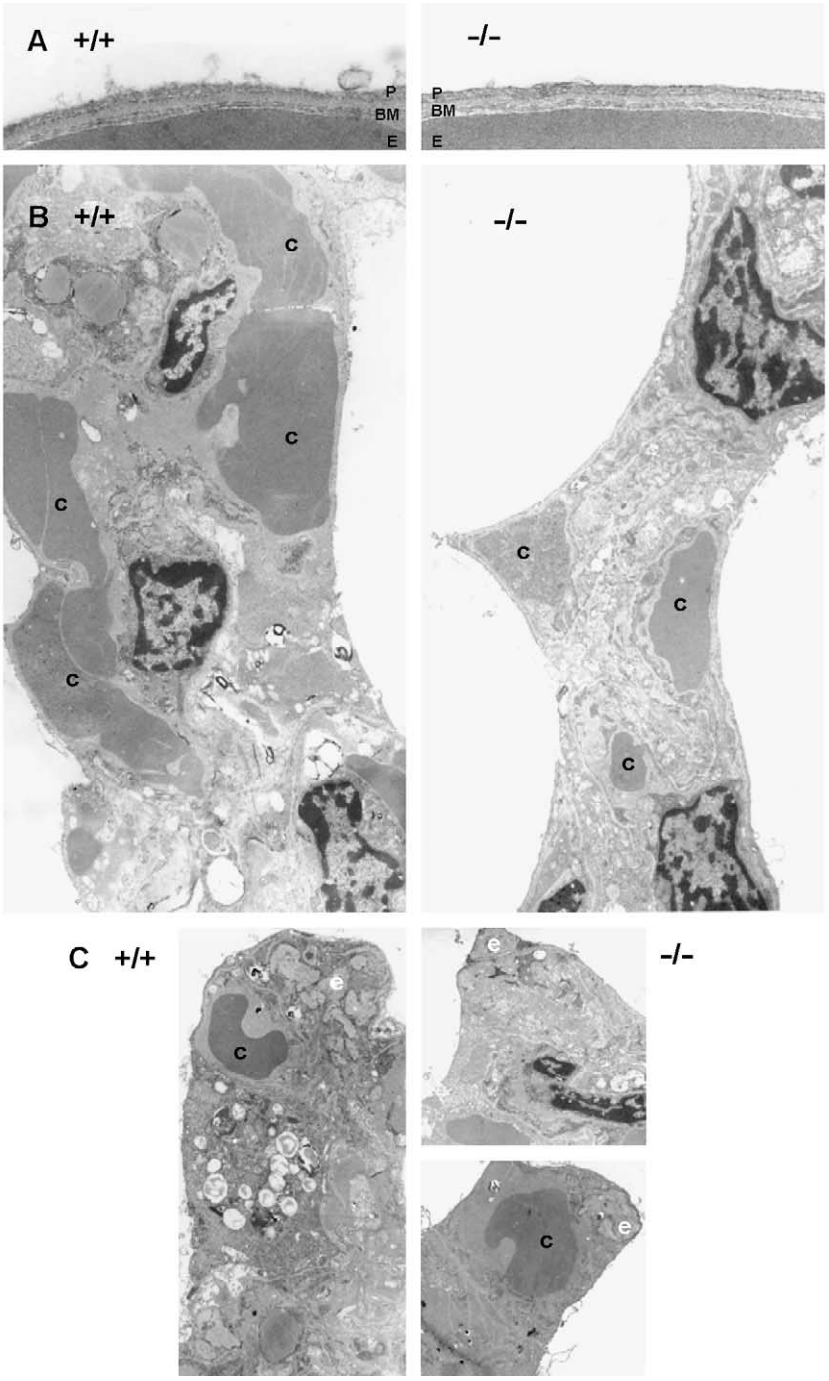

Fig. 3. Ultrastructural comparison of 2-week-old *Mmp14−/−* and +/+ lungs. (A) Basement membrane at the air–capillary interface. P, pneumocyte; BM, basement membrane; E, erythrocyte (×15,000 magnification). (B) Representative transmission electron micrographs are shown from the lung parenchyma of *Mmp14+/+* and *Mmp14−/−* mice (×8750 magnification). Capillaries occupied by erythrocytes are indicated (c). (C) A typical alveolar septum from an *Mmp14+/+* mouse (left) is compared to two septae from *Mmp14−/−* mice. Capillaries occupied by erythrocytes (c) and terminal elastic fibers (e) are indicated.

t test indicated that, although the *Mmp14−/−* mice had lower desmosine content, the difference was not statistically significant. Western blot analysis of collagen I, collagen IV (α3 chain), and collagen IV (α5 chain) content showed no differences between *Mmp14−/−* and *Mmp14+/+* lungs (data not shown). Immunostaining of basement membrane (collagen IV; Fig. 4B) revealed no significant differences. In order to examine differentiation of the surface epithelium of the lung throughout development, we carried out in situ hybridization for the detection of surfactant protein C mRNA (*Spc*), a type II epithelial cell marker. *Spc* expression patterns were comparable in normal and mutant lungs from E14.5 through postnatal development (shown in E; 16.5 days and 2 days of age in Fig. 4C), suggesting that differentiation of alveolar surface epithelium proceeded normally in *Mmp14−/−* mice. Immunostaining for markers of bronchial epithelium (Clara cell secreted protein/CCSP; data not shown) gave essentially similar results in *Mmp14−/−* and *Mmp14+/+* lungs. Markers for blood vessels [von Willebrand factor (vWF), Fig. 4D] and capillaries (CD31/PECAM-1) did not demonstrate differences between *Mmp14−/−* and *Mmp14+/+* lungs. Due to the very different architecture of *Mmp14−/−* and *Mmp14+/+* lungs and because capillaries run continuously throughout the alveolar walls, we did not quantitate CD31 staining; however, capillaries were clearly present in all alveolar walls and septae of the null mice (see also TEM data, Fig. 3). Immunostaining with smooth muscle α-actin demonstrated positively stained cells in the distal airspaces of *Mmp14−/−* null mice, including the septae, indicative of the presence of myofibroblasts (Fig. 4E).

The laminin-5 γ2 chain is a substrate for both MMP-2 and MT1-MMP, and its proteolysis promotes cell migration (Giannelli et al., 1997). Since proteolysis of the laminin-5 γ2 chain was reportedly reduced in kidney and lung basement membranes of *Mmp14−/−* mice (Koshikawa et al., 2004), we used an anti-laminin-5 γ2 chain antibody (Pyke et al., 1995) for Western blots of whole lung extract at two different ages (Fig. 4F). No alteration of laminin-5 γ2 chain processing was seen.

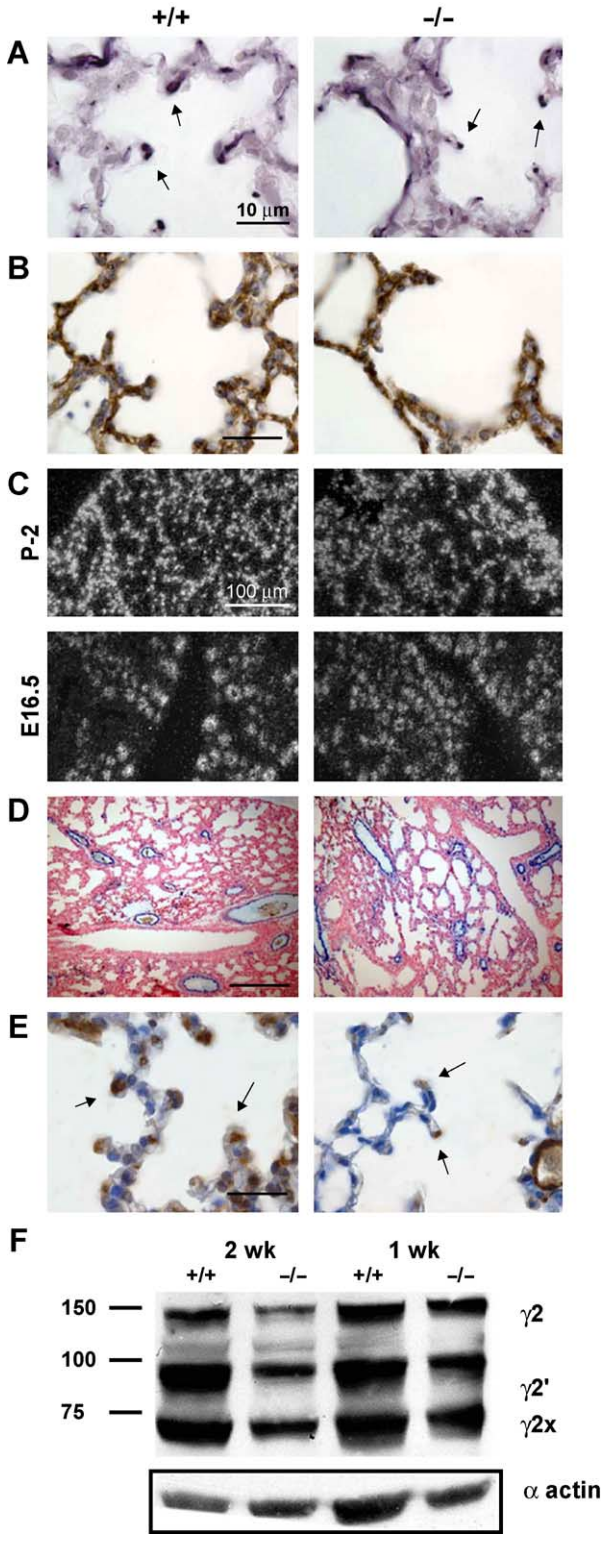

Fig. 4. Comparative analysis of *Mmp14+/+* (left) and *Mmp14−/−* (right) mice. (A) Hart's stain for elastin with arrows indicating elastic fibers in septae of 2-week-old lungs. (B) Collagen IV immunohistochemistry. Septae are indicated by arrows. (C) In situ hybridization of the surfactant protein C (Spc) gene in E16.5 and 2-day-old (P2) mice. (D) von Willebrand factor immunostaining showing mature blood vessels in 2-week-old lungs. (E) Smooth muscle α-actin stain for myofibroblasts (indicated in septal tip by arrows). (F) Western blot analysis of the laminin-5 γ2 chain using lung extracts. The age of mice and their genotype are indicated above the blot. Molecular mass markers are shown at left. The proteolytically derived fragments of laminin-5 γ2, γ2′, and γ2x are shown at right. A Western blot for α-actin is shown in the box at the bottom of the figure to indicate protein loading to each lane.

MT1-MMP is present on mouse lung endothelial cells and is required for migration and the formation of tube-like structures on matrigel

Mouse lung endothelial cells (MLEC) were isolated from *Mmp14+/+*, *Mmp14+/−*, and *Mmp14−/−* mice. First, MT1-MMP expression in these cells was analyzed by Western blotting with an anti-MT1-MMP monoclonal antibody, LEM-2/63, which recognizes the mouse protein (Galvez et al., 2001). MT1-MMP was present in MLECs from

Mmp14+/+ and *Mmp14*+/− mice (albeit reduced in the latter) but was not present in MLECs from *Mmp14*−/− mice (Fig. 5A). The role of MT1-MMP in endothelial cell migration was next studied in a transwell chamber assay (Galvez et al., 2001). Spontaneous transmigration of MLECs through matrigel-coated filters was consistently decreased in the cells lacking MT1-MMP (Fig. 5B). Interestingly, with MLEC from *Mmp14*+/− mice, the reduction was quantitatively reduced to approximately half that of the wild type (Fig. 5B). The process of formation of three-dimensional structures by null MLECs was analyzed using an in vitro assay on matrigel. The spontaneous formation of cord-like or tube-like structures from MLECs was considerably decreased in cells lacking MT1-MMP, as well as to a lesser degree in MLECs from *Mmp14*+/− mice (Fig. 5C).

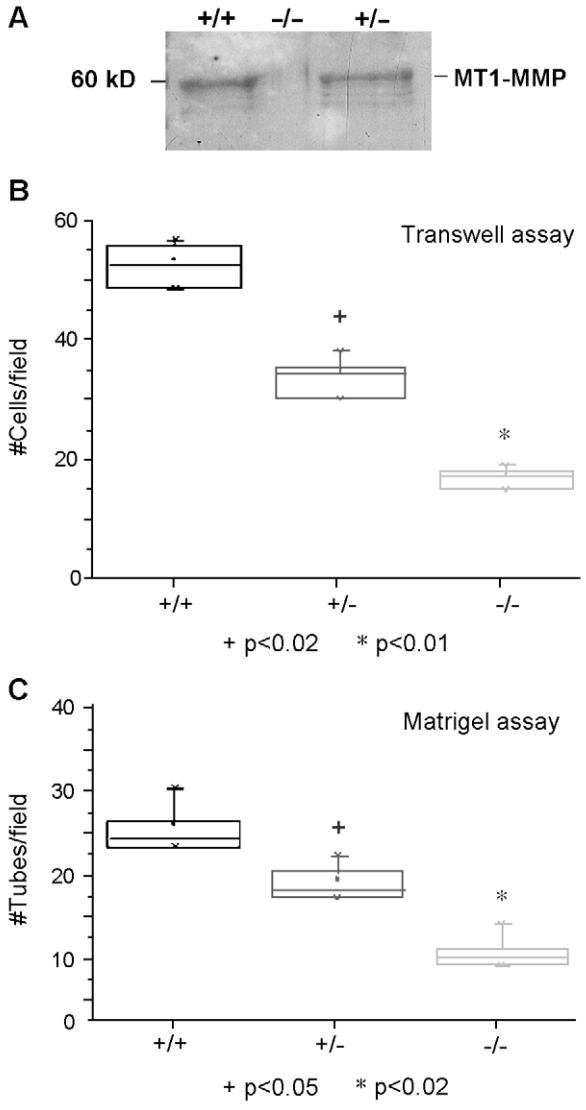

Fig. 5. *Mmp14* is required for mouse endothelial cell migration and tube formation. (A) MLEC from littermates were lysed in Laemmli sample buffer and analyzed by Western blot using anti-MT1-MMP antibody LEM-2/63. Note that *Mmp14*−/− MLEC did not express MT1-MMP. (B) MLEC from *Mmp14*+/+, *Mmp14*+/−, and *Mmp14*−/− mice were grown on Matrigel-coated 8-μm pore filters and allowed to migrate in transwell assays for 5 h. The number of cells migrating to the lower chamber was quantitated as described. (C) MLEC from *Mmp14*+/+, *Mmp14*+/−, and *Mmp14*−/− mice were seeded on Matrigel, and the number of cord or tube-like structures formed was quantitated after 4 h.

Mmp14−/− *mice have defective submandibular gland branching morphogenesis*

In situ hybridization showed prominent *Mmp14* expression in the epithelial cells of the developing submandibular gland (Fig. 6A). Two-week-old submandibular glands from *Mmp14*−/− mice were smaller than their control littermates and consistently demonstrated smaller lobules (Fig. 6B). In order to determine if submandibular gland branching morphogenesis was defective, an in vitro assay (Durbeej et al., 2001) using E13.5 submandibular gland rudiments was undertaken. At the time of dissection, each rudiment had three branch buds. Starting as early as 12 h after initiation of organ culture and throughout the subsequent period in culture, the *Mmp14*−/− submandibular glands were smaller in size and had fewer end buds (Figs. 6C, D). By 72 h, the number of end buds formed in *Mmp14*−/− submandibular glands was fewer than in their *Mmp14*+/+ littermate controls (n = 5) indicating subnormal branching (Figs. 6C, D). In addition to having fewer end buds, the mutant submandibular gland end buds also appeared dilated (Fig. 6C).

Defective activation of pro-MMP-2 is seen during lung development in Mmp14−/− *mice, but lung and submandibular gland development is normal in Mmp2*−/− *mice*

Since MT1-MMP has a role in activation of MMP-2, we analyzed MMP-2 forms in the embryonic and postnatal lung. Gelatin zymography of *Mmp14*−/− lungs at various developmental stages showed decreased activation of pro-MMP-2 in E16.5, 1-week-old, and 2-week-old lungs (Fig. 7A), but no changes in the levels or activation status of pro-MMP-9 (data not shown). However, some active MMP-2 enzyme was seen in embryonic *Mmp14*−/− lungs, suggesting that other activation mechanisms were compensating for the lack of MT1-MMP in *Mmp14*−/− lungs (Fig. 7A). We next asked whether this failure to activate pro-MMP-2 mediated the postnatal abnormalities seen in *Mmp14*−/− lungs. We analyzed the histology of 2-week-old *Mmp2*−/− mice (n = 12) relative to their +/+ littermates (n = 12) and found that they neither had anomalies similar to those in *Mmp14*−/− mice, nor did they appear abnormal in any other way (Figs. 7B, C). In *Mmp2*−/− mice, secondary septae were present and as developed as in the *Mmp2*+/+ mice. Again, to determine whether the submandibular gland changes were a consequence of defective pro-MMP-2 activation, we obtained gelatin zymograms from the submandibular gland, which showed decreased MMP-2 activation at E18.5 days of development but little activation at other time points in both *Mmp14*−/− and *Mmp14*+/+ mice

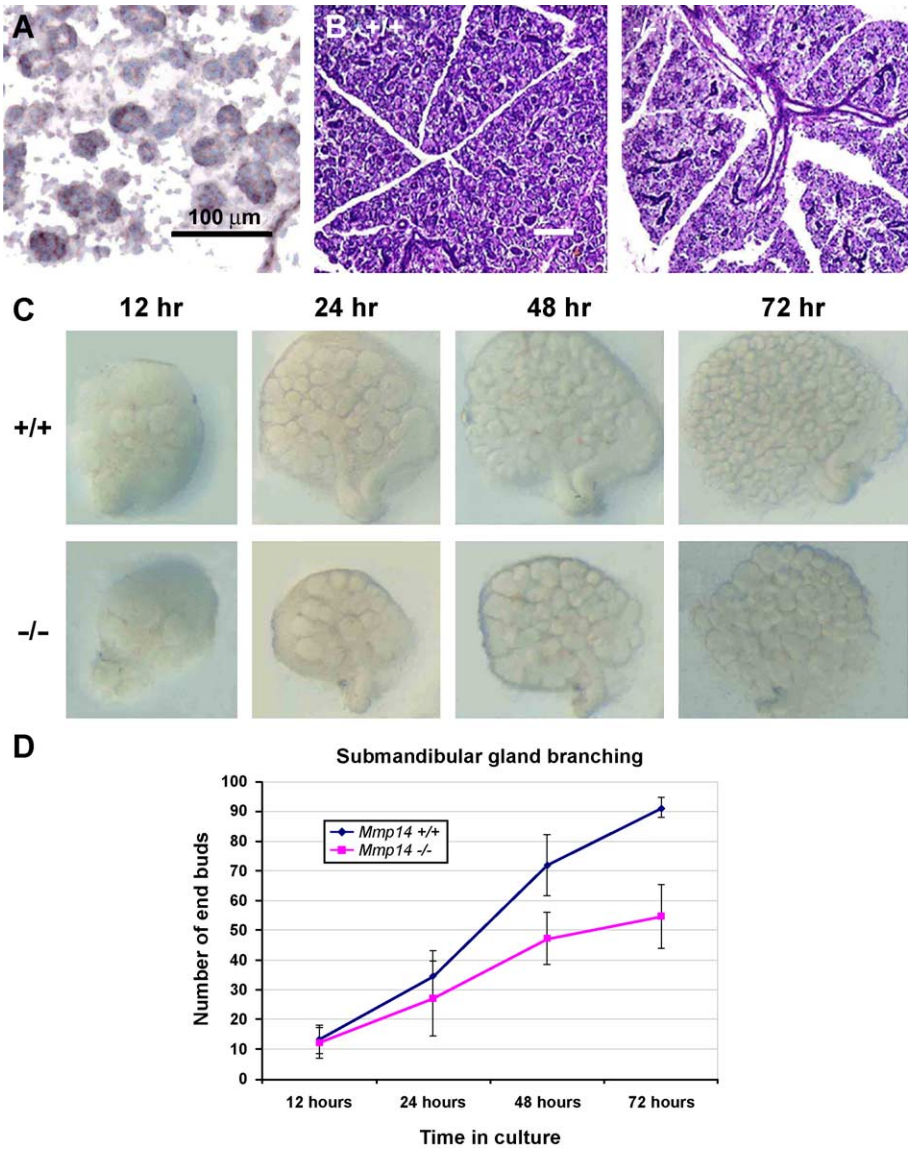

Fig. 6. Defective branching morphogenesis in *Mmp14−/−* submandibular gland rudiments. (A) Nonisotopic in situ hybridization of an E17.5 submandibular gland showing specific hybridization to ductal/glandular epithelium (magenta-stained cells). (B) Comparative H and E stained histology of 2-week-old *Mmp14+/+* (left panel) and *Mmp14−/−* (right panel) submandibular gland. (C) Representative organ culture of submandibular glands from *Mmp14+/+* (top row) and *Mmp14−/−* mice (lower row) over a period of 72-h culture in serum-free medium. (D) End buds were counted during the branching morphogenesis assay. Blue and red lines indicate *Mmp14+/+* and *Mmp14−/−*, respectively.

(Fig. 7D). However, analysis of 2-week old *Mmp2−/−* submandibular glands did not show any anomalies (Fig. 7E).

Discussion

Consistent with early studies showing that MT1-MMP is a collagenase that is prominently expressed in connective tissue cells such as osteoblasts, osteoclasts, and perichondrial, muscle, and tendon fibroblasts (Apte et al., 1997; Kinoh et al., 1996), *Mmp14−/−* mice generated independently by two groups had a strikingly abnormal musculoskeletal system (Holmbeck et al., 1999; Zhou et al., 2000). The present studies show that *Mmp14* is also expressed in epithelial organs such as the lung and submandibular gland, although the levels of expression appear lower than in developing connective tissue by in situ hybridization. Very few MMPs or their inhibitors the TIMPs are developmentally expressed in epithelia. Matrilysin-1 (MMP-7) is an exception (Dunsmore et al., 1998), but *Mmp7* null mice are developmentally normal. Instead, MMP-7 appears to regulate innate immunity (Wilson et al., 1999). *Timp3* is very highly expressed in developing lung and salivary gland epithelium (Apte et al., 1994), and *Timp3* null mice have developmental lung anomalies including defective branching morphogenesis (Gill et al., 2003; Leco et al., 2001). However, since TIMP-3 inhibits members of the MMP, ADAM, and ADAMTS protease families (Amour et al.,

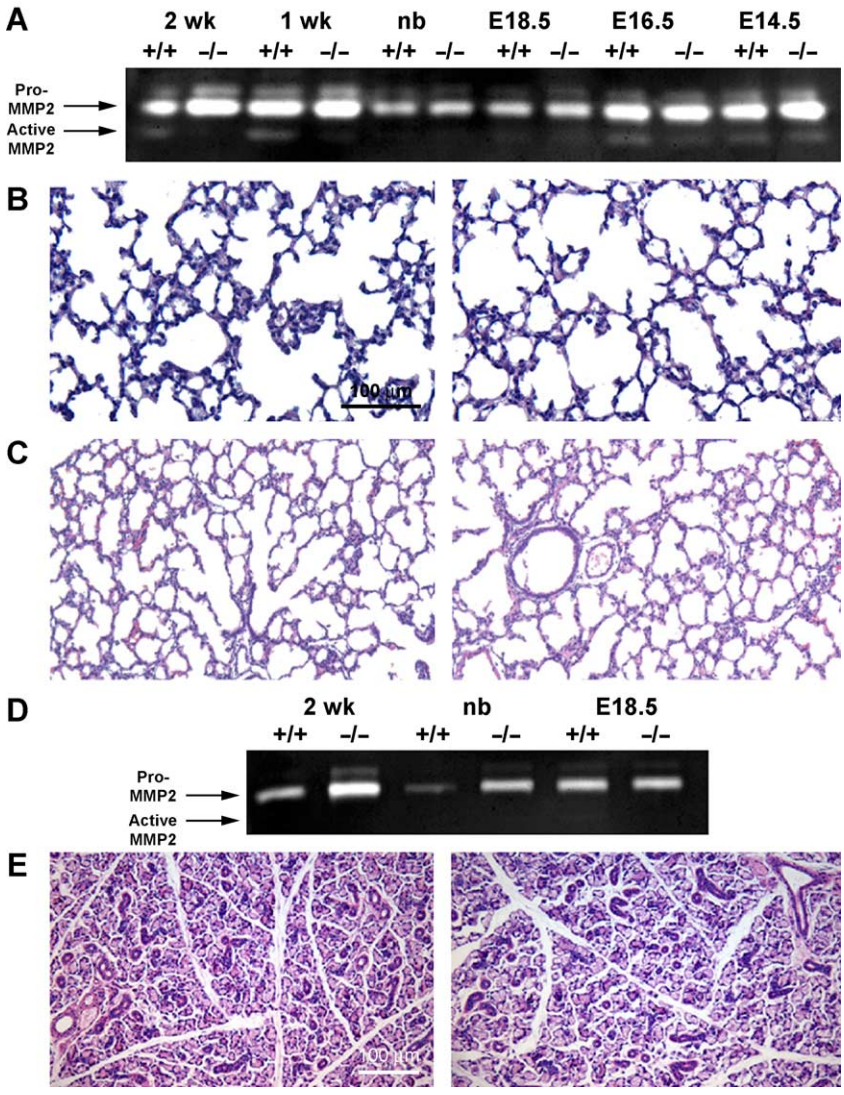

Fig. 7. MT1-MMP has a role in pro-MMP-2 activation, but *Mmp2*−/− mice do not have lung and submandibular gland anomalies. (A) Gelatin zymography of lung extracts from *Mmp14*+/+ and *Mmp14*−/− mice. Molecular identities of gelatinase activities are shown on the left, and the origin of each sample is shown above the corresponding lane. The data are representative of that obtained from three pairs of lungs at each age. (B, C) Comparative H and E-stained histology of *Mmp2*+/+ lungs (left panels) with *Mmp2*−/− lungs (right panels) at 2 weeks of age (B) and in newborn mice (C). (D) Gelatin zymography of submandibular glands from *Mmp14*+/+ and *Mmp14*−/− mice. Little activation was seen other than at E18.5 in *Mmp14*+/+ mice. (E) Comparative H and E-stained histology of 2-week-old *Mmp2*+/+ salivary gland (left panel) with *Mmp2*−/− submandibular gland (right panel).

1998; Kashiwagi et al., 2001; Loechel et al., 2000), it is difficult to implicate specific proteases in the genesis of this phenotype. Thus, although a variety of studies have implicated metalloproteases in branching of epithelia, genetic evidence implicating specific MMPs has been scarce. Recently, a comprehensive study that utilized *Mmp2* and *Mmp3* null mice demonstrated that MMP-2 and MMP-3, both of which are stromally expressed, regulated postpubertal mammary gland development (Wiseman et al., 2003). However, neither was essential for prepubertal mammary development.

To evaluate the significance of *Mmp14* expression in lung and submandibular gland, we investigated the development of these organs in *Mmp14*−/− mice. The lung presents a very complex developmental scenario in which integrated bronchial and vascular morphogenesis is required for gas–blood exchange, whereas the submandibular gland represents a simple secretory acinar gland. Since the *Mmp14*−/− mice used in this study die between 2 and 3 weeks of age (Zhou et al., 2000), we initially carried out a detailed morphological analysis at 2 weeks of age, comparing *Mmp14*−/− mice with their wild-type and heterozygous littermates. The histological appearance of the lung from the *Mmp14*−/− mice resembled that seen in emphysema, with large air spaces and thin, stretched alveolar walls. However, since the anomaly was visible at birth and was unaccompanied by an inflammatory process, it suggested a developmental, not acquired, origin.

Mouse lung development commences around E9.5 with the outgrowth of a tracheal diverticulum from the primitive

foregut (Warburton et al., 2000). Following tracheal bifurcation and further division to the primary lobar bronchi, which appears to be genetically "hard-wired," successive hierarchical branching occurs, so that a pseudoglandular structure is manifest at E12 (E9.5–16.5, the pseudoglandular stage). In the canalicular stage (E16.5–17.5), terminal sac formation and vascularization are initiated. During the terminal sac stage [E17.5 postnatal day (P)5], the number of terminal sacs increases. From P5 to P30, terminal sacs develop into mature alveoli (Warburton et al., 2000). Despite specific bronchial expression of *Mmp14* in the pseudoglandular stage, we found no defect in branching morphogenesis between 12.5 and 15.5 days of gestation using a well-characterized in vitro branching assay (Ganser et al., 1991; Serra et al., 1994; Weaver and Hogan, 2000). However, subtle morphological anomalies were seen later in embryonic development, suggesting a temporally restricted role for MT1-MMP starting in the canalicular stage and coincident with the initial stages of integration of pulmonary vasculature and branching epithelium (Warburton et al., 2000). Except for this, we concluded that MT1-MMP has a largely redundant role in branching morphogenesis of lung. In the salivary gland, however, MT1-MMP requirement was more stringent than in the lung since we noted abnormal branching in in vitro assays.

In mice, as in other mammals, including humans, lung development is incomplete at birth. The immature (prealveolar) saccules present at birth are further divided into alveoli (alveolization) by the formation and growth of septae from the saccular walls. This serves to substantially increase the surface area of the gas–blood interface. Alveolization commences shortly after birth and continues up to 30 days postnatally in mice (Warburton et al., 2000). A variety of morphological techniques led us to conclude that the principal defect in *Mmp14−/−* mice was a combined failure of postnatal saccular development and failure of secondary septae to form and extend fully into the prealveolar saccules, leading to defective alveolization. The hyperinflation of immature saccules and stretching of their walls, giving rise to a pseudoemphysematous appearance, likely represents an adaptive response.

MT1-MMP has been studied most extensively in the context of cell-surface activation of pro-MMP-2 and pro-MMP-13, and recent evidence suggests that *Mmp2−/−* mice have defective angiogenesis (Itoh et al., 1998) and impaired postpubertal mammary gland ductal development (Wiseman et al., 2003). Pro-MMP-2 activation requires TIMP-2 as an intermediary, and the essential role of TIMP-2 is underscored by the exquisite coregulation of *Mmp14* and *Timp2* in musculoskeletal tissues (Apte et al., 1997) and the lack of pro-MMP-2 activation in *Timp2* null mice (Wang et al., 2000). Accordingly, we examined the expression of *Timp2* and found it to be coexpressed with *Mmp14* in lung and salivary gland (data not shown). Furthermore, gelatin zymograms of lungs and salivary gland from *Mmp14−/−* mice suggested a role for MT1-MMP in pro-MMP-2 processing and that it was a possible mechanism for the anomalies we noted in these mice. Nevertheless, a comparable appearance of lung and salivary gland of *Mmp2−/−* mice to that seen in the *Mmp14−/−* mice was not seen. All lungs were carefully fixed under inflation to provide standardized histology. Both *Mmp14−/−* and *Mmp2−/−* mice are in a C57/BL6 background, thus eliminating strain differences. We have also considered the possibility that the *Mmp2−/−* mice may have an incompletely penetrant lung phenotype, since a previous study had suggested abnormal alveolization in a small number (15%) of *Mmp2−/−* mice (Kheradmand et al., 2002). Our studies suggest, however, that mice are born in the expected mendelian ratio, that is, without loss of a small number of mice with a severe lung phenotype. Since gelatin zymography of the *Mmp2−/−* mice showed no detectable MMP-2 activity (data not shown), *Mmp14−/−* mice would not in fact have as severe a deficiency of active MMP-2 as the *Mmp2−/−* mice.

We therefore concluded that the partial loss of pro-MMP-2 activation seen in *Mmp14* null mice is not the underlying mechanism for the abnormalities seen in the lung and salivary gland. MT1-MMP has also been implicated in activation of the collagenase pro-MMP-13 (Knauper et al., 2002). However, unpublished studies of *Mmp13−/−* mice (personal communication of Dr. Stephen Krane, Massachusetts General Hospital) indicate that they do not have abnormal pulmonary histology.

What then could be responsible for defective alveolization in *Mmp14−/−* mice? The data summarized in Table 1 suggest no significant molecular differences between *Mmp14−/−* and *Mmp14+/+* mice. Neither accumulation of interstitial collagen nor thickening of basement membrane was seen by TEM or immunohistochemistry. In addition, laminin-5 processing was unaffected, suggesting that failure of collagen I or basement membrane proteolysis did not underlie the phenotype. We detected normal cell differentiation in the *Mmp14−/−* mice. There was a well-defined elastin network throughout the lung. Thus, although the phenotype was somewhat similar to that of elastin-deficient mice (Wendel et al., 2000), deficient elastogenesis did not explain the anomalies. We also considered that defective release or activation of ECM-bound growth factors could give rise to the anomalies noted. Although *Egfr−/−* mice have defective alveolization (Miettinen et al., 1995), they also have defective branching morphogenesis in lung explants (Miettinen et al., 1997), which was not seen in *Mmp14−/−* mice. *Pdgfa−/−* mice have a pseudo-emphysematous phenotype that superficially resembles that of the *Mmp14−/−* mice and is caused by failed septation (Bostrom et al., 1996). PDGF-A is essential for myofibroblast development, and these cells are absent in *Pdgfa−/−* lungs (Bostrom et al., 1996). However, smooth muscle α-actin-positive cells (presumed myofibroblasts) were clearly present in 2-week-old *Mmp14−/−* mice, including a cell consistently present at the tip of the septum.

Two substantive considerations led us to investigate defective angiogenesis as an underlying mechanism of the

Table 1
Comparison of molecular parameters evaluated in the lungs of 2-week-old *Mmp14*+/+ and *Mmp14*−/− mice

Target	Assay	Outcome
Collagen I	Immunoblot	Identical bands of similar intensity
Collagen IV α3	Immunoblot	Identical bands of similar intensity
Collagen IV α5	Immunoblot	Identical bands of similar intensity
Laminin-5 γ2	Immunoblot	Identical bands of similar intensity
Surfactant protein C	In situ hybridization	Similar distribution
Clara cell-secreted protein	Immunohistochemistry	Similar distribution and intensity
Collagen IV	Immunohistochemistry	Similar distribution and intensity
PECAM-1/CD31	Immunohistochemistry	Similar distribution and intensity
Surfactant protein B	Immunohistochemistry	Similar distribution and intensity
von Willebrand factor	Immunohistochemistry	Similar distribution and intensity
Elastin	Modified Hart's stain	Similar distribution and intensity[a]

[a] Owing to the stretched alveolar wall in *Mmp14*−/− mice, elastic fibers appeared to be attenuated but were present in all septae.

defective alveolization. The first was the critical role of angiogenesis in septation and the second related to the emerging role for MT1-MMP in diverse aspects of angiogenesis. Early morphological studies demonstrated the intimate involvement of a new capillary loop in pulmonary septal growth (Burri, 1974, 1984). Recent experimental work showed that the anti-angiogenic agents, fumagillin and thalidomide, and a chemical inhibitor of the vascular endothelial growth factor (VEGF) receptor (Su-5416) reduced alveolization in rats during the first 2 weeks of life (Jakkula et al., 2000; Kasahara et al., 2000). Administration of mFlt(1-3)-IgG (a soluble VEGF receptor that acts as a decoy for the circulating VEGF) shortly after birth resulted in severe dwarfism and anomalies in multiple epithelial organs such as liver, kidney, and lung (Gerber et al., 1999). The lungs in mFlt(1-3)-IgG-treated mice appear histologically similar to those of *Mmp14*−/− mice showing large air saccules and poor septal growth (Gerber et al., 1999).

MT1-MMP has a compelling connection with angiogenesis. Transcriptional upregulation of MT1-MMP occurs as an Egr-1-mediated early event during the initial stages of formation of three-dimensional structures and capillary tubes from microvascular endothelial cells (Haas et al., 1998, 1999). The significance of this may not be related to ECM proteolysis alone, since it has been demonstrated that MT1-MMP upregulates VEGF expression in endothelial cells (Sounni et al., 2002, 2004), although the underlying mechanisms are unclear. Previous characterization of the *Mmp14*−/− mice demonstrated impaired vascular invasion of some primary and secondary centers of ossification in the developing skeleton (Holmbeck et al., 1999; Zhou et al., 2000). In addition, we had used a corneal neovascularization assay to demonstrate the lack of an angiogenic response to FGF-2 in *Mmp14*−/− mice (Zhou et al., 2000). It is also noteworthy that the emergence of lung anomalies in *Mmp14*−/− mice occurred coincidentally with the initial vascularization of the lung (around E16.5) (Warburton et al., 2000).

Accordingly, we asked if MLECs from *Mmp14*−/− mice at 1 week of age behaved differently from those isolated from wild-type *Mmp14* littermates. Our studies show that MLECs not only express MT1-MMP, but that those from *Mmp14*−/− mice are indeed defective in cell migration and tube formation, two of the essential prerequisites for angiogenesis. PECAM/CD31 stained cells were seen in all alveolar walls, as expected, and capillaries were seen on TEM throughout the lung and in each septum. We suggest that impairment of migration and tube formation restricts their ability to grow further into the developing septum postnatally and is rate-limiting for further lung development. A reduction of angiogenic potential in *Mmp14*+/− mice is plausible but did not affect normal development, since these mice (and their lungs) were indistinguishable from the wild-type mice. Until selective targeted deletion of *Mmp14* in endothelial cells is achieved, it will not be possible to evaluate whether impaired angiogenesis is the only mechanism underlying defective alveolization. For instance, we note that myofibroblasts are present in the lungs of *Mmp14*−/− mice, but we have not excluded possibility that their migration might also be defective.

In conclusion, the data presented here support a significant role for MT1-MMP in morphogenesis of epithelial tissues through studies of two representative organs. The contrasting roles in each are evident from the postnatal defect in lung development with normal branching morphogenesis, whereas the defect in submandibular gland development is embryological and affects branching morphogenesis. Despite these differences, our studies make the important point that the underlying mechanisms are independent of pro-MMP-2 activation and, at least in the lung, may involve a restriction of angiogenesis. The data support an emerging model in which angiogenesis is essential for the growth and maintenance of pulmonary parenchymal mass (Gerber et al., 1999; Jakkula et al., 2000; Kasahara et al., 2000; Shapiro, 2000; Tuder et al., 2000, 2003). We propose that the "emphysema-like" morphology of *Mmp14*−/− lungs represents an arrest of postnatal lung development and is the maximal parenchymal mass that can be attained and supported in the presence of reduced endothelial capillary-forming ability.

Acknowledgments

We thank Dr. Shigeyoshi Itohara (Laboratory for Behavorial Genetics, Brain Research Institute, RIKEN, Japan) and Dr. Michael Shipley (Washington University,

St. Louis) for helping to establish *Mmp2−/−* mouse lines. Dr. Rosa Serra (University of Alabama-Birmingham) and Dr. Robert Somerville (Cleveland Clinic) provided technical advice and valuable discussion. This research was supported by NIH AR47074 (to S.A.) and RGC CERG grant 2110204672 (to Z.Z.).

References

Affolter, M., Bellusci, S., Itoh, N., Shilo, B., Thiery, J.P., Werb, Z., 2003. Tube or not tube: remodeling epithelial tissues by branching morphogenesis. Dev. Cell 4, 11–18.

Albrecht, U., Eichele, G., Helms, J.A., Lu, H.C., 1997. Molecular and Cellular Methods in Developmental Toxicology. CRC Press Inc, Boca Raton, FL.

Alexander, C.M., Howard, E.W., Bissell, M.J., Werb, Z., 1996. Rescue of mammary epithelial cell apoptosis and entactin degradation by a tissue inhibitor of metalloproteinases-1 transgene. J. Cell Biol. 135, 1669–1677.

Amour, A., Slocombe, P.M., Webster, A., Butler, M., Knight, C.G., Smith, B.J., Stephens, P.E., Shelley, C., Hutton, M., Knauper, V., Docherty, A.J., Murphy, G., 1998. TNF-alpha converting enzyme (TACE) is inhibited by TIMP-3. FEBS Lett. 435, 39–44.

Apte, S.S., Hayashi, K., Seldin, M.F., Mattei, M.G., Hayashi, M., Olsen, B.R., 1994. Gene encoding a novel murine tissue inhibitor of metalloproteinases (TIMP), TIMP-3, is expressed in developing mouse epithelia, cartilage, and muscle, and is located on mouse chromosome 10. Dev. Dyn. 200, 177–197.

Apte, S.S., Fukai, N., Beier, D.R., Olsen, B.R., 1997. The matrix metalloproteinase-14 (MMP-14) gene is structurally distinct from other MMP genes and is co-expressed with the TIMP-2 gene during mouse embryogenesis. J. Biol. Chem. 272, 25511–25517.

Blavier, L., Delaisse, J.M., 1995. Matrix metalloproteinases are obligatory for the migration of preosteoclasts to the developing marrow cavity of primitive long bones. J. Cell Sci. 108 (Pt. 12), 3649–3659.

Bostrom, H., Willetts, K., Pekny, M., Leveen, P., Lindahl, P., Hedstrand, H., Pekna, M., Hellstrom, M., Gebre-Medhin, S., Schalling, M., Nilsson, M., Kurland, S., Tornell, J., Heath, J.K., Betsholtz, C., 1996. PDGF-A signaling is a critical event in lung alveolar myofibroblast development and alveogenesis. Cell 85, 863–873.

Burri, P.H., 1974. The postnatal growth of the rat lung. 3. Morphology. Anat. Rec. 180, 77–98.

Burri, P.H., 1984. Fetal and postnatal development of the lung. Annu. Rev., Physiol. 46, 617–628.

D'Armiento, J., Dalal, S.S., Okada, Y., Berg, R.A., Chada, K., 1992. Collagenase expression in the lungs of transgenic mice causes pulmonary emphysema. Cell 71, 955–961.

Deterding, R.R., Shannon, J.M., 1995. Proliferation and differentiation of fetal rat pulmonary epithelium in the absence of mesenchyme. J. Clin. Invest. 95, 2963–2972.

Dunsmore, S.W., Saarialho-Kere, U.K., Roby, J.D., Wilson, C.L., Matrisian, L.M., Welgus, H.G., Parks, W.C., 1998. Matrilysin expression and function in airway epithelium. J. Clin. Invest. 102, 1321–1331.

Durbeej, M., Talts, J.F., Henry, M.D., Yurchenco, P.D., Campbell, K.P., Ekblom, P., 2001. Dystroglycan binding to laminin alpha1LG4 module influences epithelial morphogenesis of salivary gland and lung in vitro. Differentiation 69, 121–134.

Galvez, B.G., Matias-Roman, S., Albar, J.P., Sanchez-Madrid, F., Arroyo, A.G., 2001. Membrane type 1-matrix metalloproteinase is activated during migration of human endothelial cells and modulates endothelial motility and matrix remodeling. J. Biol. Chem. 276, 37491–37500.

Ganser, G.L., Stricklin, G.P., Matrisian, L.M., 1991. EGF and TGF alpha influence in vitro lung development by the induction of matrix-degrading metalloproteinases. Int. J. Dev. Biol. 35, 453–461.

Gerber, H.P., Hillan, K.J., Ryan, A.M., Kowalski, J., Keller, G.A., Rangell, L., Wright, B.D., Radtke, F., Aguet, M., Ferrara, N., 1999. VEGF is required for growth and survival in neonatal mice. Development 126, 1149–1159.

Giannelli, G., Falk-Marzillier, J., Schiraldi, O., Stetler-Stevenson, W.G., Quaranta, V., 1997. Induction of cell migration by matrix metalloprotease-2 cleavage of laminin-5. Science 277, 225–228.

Gill, S.E., Pape, M.C., Khokha, R., Watson, A.J., Leco, K.J., 2003. A null mutation for tissue inhibitor of metalloproteinases-3 (Timp-3) impairs murine bronchiole branching morphogenesis. Dev. Biol. 261, 313–323.

Haas, T.L., Davis, S.J., Madri, J.A., 1998. Three-dimensional type I collagen lattices induce coordinate expression of matrix metalloproteinases MT1-MMP and MMP-2 in microvascular endothelial cells. J. Biol. Chem. 273, 3604–3610.

Haas, T.L., Stitelman, D., Davis, S.J., Apte, S.S., Madri, J.A., 1999. Egr-1 mediates extracellular matrix-driven transcription of membrane type 1 matrix metalloproteinase in endothelium. J. Biol. Chem. 274, 22679–22685.

Holmbeck, K., Bianco, P., Caterina, J., Yamada, S., Kromer, M., Kuznetsov, S.A., Mankani, M., Robey, P.G., Poole, A.R., Pidoux, I., Ward, J.M., Birkedal-Hansen, H., 1999. MT1-MMP-deficient mice develop dwarfism, osteopenia, arthritis, and connective tissue disease due to inadequate collagen turnover. Cell 99, 81–92.

Hotary, K.B., Yana, I., Sabeh, F., Li, X.Y., Holmbeck, K., Birkedal-Hansen, H., Allen, E.D., Hiraoka, N., Weiss, S.J., 2002. Matrix metalloproteinases (MMPs) regulate fibrin-invasive activity via MT1-MMP-dependent and -independent processes. J. Exp. Med. 195, 295–308.

Itoh, T., Ikeda, T., Gomi, H., Nakao, S., Suzuki, T., Itohara, S., 1997. Unaltered secretion of beta-amyloid precursor protein in gelatinase A (matrix metalloproteinase 2)-deficient mice. J. Biol. Chem. 272, 22389–22392.

Itoh, T., Tanioka, M., Yoshida, H., Yoshioka, T., Nishimoto, H., Itohara, S., 1998. Reduced angiogenesis and tumor progression in gelatinase A-deficient mice. Cancer Res. 58, 1048–1051.

Jakkula, M., Le Cras, T.D., Gebb, S., Hirth, K.P., Tuder, R.M., Voelkel, N.F., Abman, S.H., 2000. Inhibition of angiogenesis decreases alveolarization in the developing rat lung. Am. J. Physiol.: Lung Cell Mol. Physiol. 279, L600–L607.

Johansson, N., Saarialho-Kere, U., Airola, K., Herva, R., Nissinen, L., Westermarck, J., Vuorio, E., Heino, J., Kahari, V.M., 1997. Collagenase-3 (MMP-13) is expressed by hypertrophic chondrocytes, periosteal cells, and osteoblasts during human fetal bone development. Dev. Dyn. 208, 387–397.

Kanwar, Y.S., Wada, J., Lin, S., Danesh, F.R., Chugh, S.S., Yang, Q., Banerjee, T., Lomasney, J.W., 2004. Update of extracellular matrix, its receptors, and cell adhesion molecules in mammalian nephrogenesis. Am. J. Physiol.: Renal Physiol. 286, F202–F215.

Kasahara, Y., Tuder, R.M., Taraseviciene-Stewart, L., Le Cras, T.D., Abman, S., Hirth, P.K., Waltenberger, J., Voelkel, N.F., 2000. Inhibition of VEGF receptors causes lung cell apoptosis and emphysema. J. Clin. Invest. 106, 1311–1319.

Kashiwagi, M., Tortorella, M., Nagase, H., Brew, K., 2001. TIMP-3 is a potent inhibitor of aggrecanase 1 (ADAM-TS4) and aggrecanase 2 (ADAM-TS5). J. Biol. Chem. 276, 12501–12504.

Kheradmand, F., Rishi, K., Werb, Z., 2002. Signaling through EGF receptor controls lung morphogenesis in part by regulating MT1-MMP-mediated activation of gelatinase A/MMP-2. J. Cell Sci. 115, 839–848.

Kinoh, H., Sato, H., Tsunezuka, Y., Takino, T., Kawashima, A., Okada, Y., Seiki, M., 1996. MT-MMP, the cell surface activator of proMMP-2 (pro-gelatinase A), is expressed with its substrate in mouse tissue during embryogenesis. J. Cell Sci. 109 (Pt. 5), 953–959.

Knauper, V.B.L., Worley, J.R., Soloway, P., Patterson, M.L., Murphy, G., 2002. Cellular activation of proMMP-13 by MT1-MMP depends on the C-terminal domain of MMP-13. FEBS Lett. 532, 127–130.

Koshikawa, N., Schenk, S., Moeckel, G., Sharabi, A., Miyazaki, K., Gardner, H., Zent, R., Quaranta, V., 2004. Proteolytic processing of

laminin-5 by MT1-MMP in tissues and its effects on epithelial cell morphology. FASEB J. 18, 364–366.
Leco, K.J., Waterhouse, P., Sanchez, O.H., Gowing, K.L., Poole, A.R., Wakeham, A., Mak, T.W., Khokha, R., 2001. Spontaneous air space enlargement in the lungs of mice lacking tissue inhibitor of metalloproteinases-3 (TIMP-3). J. Clin. Invest. 108, 817–829.
Loechel, F., Fox, J.W., Murphy, G., Albrechtsen, R., Wewer, U.M., 2000. ADAM 12-S cleaves IGFBP-3 and IGFBP-5 and is inhibited by TIMP-3. Biochem. Biophys. Res. Commun. 278, 511–515.
Martignetti, J.A., Aqeel, A.A., Sewairi, W.A., Boumah, C.E., Kambouris, M., Mayouf, S.A., Sheth, K.V., Eid, W.A., Dowling, O., Harris, J., Glucksman, M.J., Bahabri, S., Meyer, B.F., Desnick, R.J., 2001. Mutation of the matrix metalloproteinase 2 gene (MMP2) causes a multicentric osteolysis and arthritis syndrome. Nat. Genet. 28, 261–265.
Miettinen, P.J., Berger, J.E., Meneses, J., Phung, Y., Pedersen, R.A., Werb, Z., Derynck, R., 1995. Epithelial immaturity and multiorgan failure in mice lacking epidermal growth factor receptor. Nature 376, 337–341.
Miettinen, P.J., Warburton, D., Bu, D., Zhao, J.S., Berger, J.E., Minoo, P., Koivisto, T., Allen, L., Dobbs, L., Werb, Z., Derynck, R., 1997. Impaired lung branching morphogenesis in the absence of functional EGF receptor. Dev. Biol. 186, 224–236.
Ohuchi, E., Imai, K., Fujii, Y., Sato, H., Seiki, M., Okada, Y., 1997. Membrane type 1 matrix metalloproteinase digests interstitial collagen and other extracellular matrix macromolecules. J. Biol. Chem. 272, 2446–2451.
Parks, W.C., Shapiro, S.D., 2001. Matrix metalloproteinases in lung biology. Respir. Res. 2, 10–19.
Pyke, C., Salo, S., Ralfkiaer, E., Romer, J., Dano, K., Tryggvason, K., 1995. Laminin-5 is a marker of invading cancer cells in some human carcinomas and is coexpressed with the receptor for urokinase plasminogen activator in budding cancer cells in colon adenocarcinomas. Cancer Res. 55, 4132–4139.
Sato, H., Takino, T., Okada, Y., Cao, J., Shinagawa, A., Yamamoto, E., Seiki, M., 1994. A matrix metalloproteinase expressed on the surface of invasive tumor cells. Nature 370, 61–65.
Sato, H., K.T., Takino, T., Nakayama, K., Seiki, M., 1996. Activation of a recombinant membrane type 1-matrix metalloproteinase (MT1-MMP) by furin and its interaction with tissue inhibitor of metalloproteinases (TIMP)-2. FEBS Lett. 393, 101–104.
Serra, R., Pelton, R.W., Moses, H.L., 1994. TGF beta 1 inhibits branching morphogenesis and *N-myc* expression in lung bud organ cultures. Development 120, 2153–2161.
Shapiro, S.D., 2000. Vascular atrophy and VEGFR-2 signaling: old theories of pulmonary emphysema meet new data. J. Clin. Invest. 106, 1309–1310.
Simian, M., Hirai, Y., Navre, M., Werb, Z., Lochter, A., Bissell, M.J., 2001. The interplay of matrix metalloproteinases, morphogens and growth factors is necessary for branching of mammary epithelial cells. Development 128, 3117–3131.
Somerville, R.P., Oblander, S.A., Apte, S.S., 2003. Matrix metalloproteinases: old dogs with new tricks. Genome Biol. 4, 216.
Sounni, N.E., Devy, L., Hajitou, A., Frankenne, F., Munaut, C., Gilles, C., Deroanne, C., Thompson, E.W., Foidart, J.M., Noel, A., 2002. MT1-MMP expression promotes tumor growth and angiogenesis through an up-regulation of vascular endothelial growth factor expression. FASEB J. 16, 555–564.
Sounni, N.E., Roghi, C., Chabottaux, V., Janssen, M., Munaut, C., Maquoi, E., Galvez, B.G., Gilles, C., Frankenne, F., Murphy, G., Foidart, J.M., Noel, A., 2004. Up-regulation of VEGF-A by active MT1-MMP through activation of Src-tyrosine kinases. J. Biol. Chem. 279, 13564–13574.
Starcher, B., Conrad, M., 1995. A role for neutrophil elastase in solar elastosis. Ciba Found. Symp. 192, 338–346. Discussion 346–347.
Strongin, A.Y., Collier, I., Bannikov, G., Marmer, B.L., Grant, G.A., Goldberg, G.I., 1995. Mechanism of cell surface activation of 72-kDa type IV collagenase. Isolation of the activated form of the membrane metalloprotease. J. Biol. Chem. 270, 5331–5338.
Sympson, C.J., Talhouk, R.S., Alexander, C.M., Chin, J.R., Clift, S.M., Bissell, M.J., Werb, Z., 1994. Targeted expression of stromelysin-1 in mammary gland provides evidence for a role of proteinases in branching morphogenesis and the requirement for an intact basement membrane for tissue-specific gene expression. J. Cell Biol. 125, 681–693.
Tuder, R.M., Kasahara, Y., Voelkel, N.F., 2000. Inhibition of vascular endothelial growth factor receptors causes emphysema in rats. Chest 117, 281S.
Tuder, R.M., Zhen, L., Cho, C.Y., Taraseviciene-Stewart, L., Kasahara, Y., Salvemini, D., Voelkel, N.F., Flores, S.C., 2003. Oxidative stress and apoptosis interact and cause emphysema due to vascular endothelial growth factor receptor blockade. Am. J. Respir. Cell Mol. Biol. 29, 88–97.
Wang, Z., Juttermann, R., Soloway, P.D., 2000. TIMP-2 is required for efficient activation of proMMP-2 in vivo. J. Biol. Chem. 275, 26411–26415.
Warburton, D., Schwarz, M., Tefft, D., Flores-Delgado, G., Anderson, K.D., Cardoso, W.V., 2000. The molecular basis of lung morphogenesis. Mech. Dev. 92, 55–81.
Weaver, M., Dunn, N.R., Hogan, B.L., 2000. Bmp4 and Fgf10 play opposing roles during lung bud morphogenesis. Development 127, 2695–2704.
Wendel, D.P., Taylor, D.G., Albertine, K.H., Keating, M.T., Li, D.Y., 2000. Impaired distal airway development in mice lacking elastin. Am. J. Respir. Cell Mol. Biol. 23, 320–326.
Werb, Z., 1997. ECM and cell surface proteolysis: regulating cellular ecology. Cell 91, 439–442.
Wilson, C.L., Ouellette, A.J., Satchell, D.P., Ayabe, T., Lopez-Boado, Y.S., Stratman, J.L., Hultgren, S.J., Matrisian, L.M., Parks, W.C., 1999. Regulation of intestinal alpha-defensin activation by the metalloproteinase matrilysin in innate host defense. Science 286, 113–117.
Wiseman, B.S., Sternlicht, M.D., Lund, L.R., Alexander, C.M., Mott, J., Bissell, M.J., Soloway, P., Itohara, S., Werb, Z., 2003. Site-specific inductive and inhibitory activities of MMP-2 and MMP-3 orchestrate mammary gland branching morphogenesis. J. Cell Biol. 162, 1123–1133.
Witty, J.P., Wright, J.H., Matrisian, L.M., 1995. Matrix metalloproteinases are expressed during ductal and alveolar mammary morphogenesis, and misregulation of stromelysin-1 in transgenic mice induces unscheduled alveolar development. Mol. Biol. Cell 6, 1287–1303.
Yana, I., Seiki, M., 2002. MT-MMPs play pivotal roles in cancer dissemination. Clin. Exp. Metastasis 19, 209–215.
Yana, I., Weiss, S.J., 2000. Regulation of membrane type-1 matrix metalloproteinase activation by proprotein convertases. Mol. Biol. Cell 11, 2387–2401.
Zhou, Z., Apte, S.S., Soininen, R., Cao, R., Baaklini, G.Y., Rauser, R.W., Wang, J., Cao, Y., Tryggvason, K., 2000. Impaired endochondral ossification and angiogenesis in mice deficient in membrane-type matrix metalloproteinase I. Proc. Natl. Acad. Sci. U. S. A. 97, 4052–4057.
Zucker, S., Pei, D., Cao, J., Lopez-Otin, C., 2003. Membrane type-matrix metalloproteinases (MT-MMP). Curr. Top. Dev. Biol. 54, 1–74.